Science Advances
AAAS

Supplementary Materials for

Positive interactions are common among culturable bacteria

Jared Kehe, Anthony Ortiz, Anthony Kulesa, Jeff Gore,
Paul C. Blainey*, Jonathan Friedman*

*Corresponding author. Email: pblainey@broadinstitute.org (P.C.B.); yonatan.friedman@mail.huji.ac.il (J.F.)

Published 5 November 2021, *Sci. Adv.* **7**, eabi7159 (2021)
DOI: 10.1126/sciadv.abi7159

The PDF file includes:

Materials and Methods
Figs. S1 to S22
Tables S1 and S2
Legend for data S1

Other Supplementary Material for this manuscript includes the following:

Data S1

Materials and Methods

kChip design

All kChips were designed in AutoCAD (Autodesk). Each kChip (62 mm × 72 cm) possessed the following features: (a) An array of ~34,000 microwells (50 mm × 60 mm microfluidic field) where each microwell (slot-shaped, 148.2 μm across, 296.4 μm long) was designed to group $k = 2$ droplets and arrayed with 50-μm inter-microwell spacing; (b) Internal posts within these microwells designed to (i) reduce overfilling (via droplets squeezing into a microwell), (ii) reduce underfilling (via droplets exiting microwells due to the oil flow associated with the kChip loading procedure), and (iii) inhibit the entry of large droplets inherent to the droplet pool (*i.e.* a low-pass size filter); (c) A series of 30 90-μm deep moat-like slots designed to trap small droplets (*i.e.* a high-pass size filter) spaced 50 μm apart from each other, 400 μm from the onset of the microfluidic field, and 3 mm inset from the edge of the kChip; and (d) A loading slot into which droplets were injected via micropipette.

The optimal microwell geometries and distances between posts was optimized based on the choice of medium and concentration of fluorosurfactant (RAN Biotech 008 FluoroSurfactant), which we have previously shown affect the size of droplets produced by a Bio-Rad QX200 Droplet Generator, and by extension, droplet grouping and merging performance (*33*).

Photomasks were generated from AutoCAD designs (FineLine Imaging). kChip designs were then fabricated to 110-120 μm feature height using photolithography on silicon wafers (Microchem SU8-2050). Microwells produced from this feature height were found to best trap droplets in a monolayer, as deeper features can allow droplets to stack causing loading of an undesired number of droplets (*33*). These wafers were then embedded into custom molds to create PDMS (Dow Corning Sylgard) kChips by soft lithography with consistent thickness (0.635 cm) and droplet-loading slot location and size. The side of the kChip that contained microwell features was then coated with 1.5 μm parylene C by vapor deposition (Paratronix) to inhibit water loss from droplets and stiffen the kChip to prevent interior collapse during droplet loading.

kChip coculture construction

The following steps were performed for each kChip, with 6 kChips run in sequence per day (for a total of 24 kChip run over 4 days, with 2 kChips repeated due to poor droplet loading). As previously described, a single labeled strain was projected to all unlabeled strains, each labeled/unlabeled input and each carbon source input received a unique color code, droplets were made from all inputs, and all droplets were pooled together (**Fig 1A**, Steps 1-2). With the assistance of a loading apparatus (**fig S2A**), the droplets were loaded onto a kChip in one pipetting step (**Fig 1A**, Step 3).

A kChip loading apparatus, which was required to load droplets into microwells, consisted of a "loader top" and "loader base" (**fig S1A**). The loader base held in place a piece of custom-cut glass (Brain Research Laboratories; 1.2 mm thickness) made hydrophobic via pretreatment with Aquapel. The top side of the kChip, which was not coated with parylene, spontaneously formed a seal with the loader top. Four neodymium magnet pairs were oriented such that the two acrylic pieces repelled each other. Working against this repulsive force, the loader top was lowered toward the loader base via tightening nuts until the desired standoff between the glass and kChip was attained (~500-700 μm) to create a space for flow under the microwells. Via an open slot passing through the loader top and kChip, the flow space was pre-wetted with an injection of oil (~3 mL to fill the entirety of the flow space) followed by the pooled droplets. Each kChip consisted of an array of microwells, each designed to randomly group a specific number of droplets. Here we used

only "$k = 2$" microwells that each group two droplets. Buoyant in the surrounding oil, the droplets were distributed around the flow space via tilting the loading apparatus. After the droplets had passed through the flow space and entered the $k = 2$ microwells, additional oil (no fluorosurfactant) was flushed through the device to wash away excess droplets and fluorosurfactant. The kChip, coupled to the top piece, was removed, and sealed with a transparent PCR film (*35*), limiting inter-microwell crosstalk (*34*). The edges of the film were trimmed off. A second set of four neodymium magnets were used to couple to the top piece/kChip to a microscope stage adapter.

Setting up the kChip loading apparatus in preparation to receive droplets took 5-10 minutes and was completed ahead of time. The remaining setup time was ~30 minutes: Droplet making took ~3 minutes per eight inputs on the Bio-Rad QX200, droplet pooling and mixing took ~5 minutes, loading the kChip took ~5-10 minutes, and scanning the kChip took ~12-15 minutes.

The kChip was scanned initially at 2X magnification to identify the droplets in each microwell from their color codes (**Fig S1B**). Droplets were then merged within their microwells via exposure to an alternating current (AC) electric field (4.5 MHz, 10,000-45,000 volts) underneath the PCR film (**Fig 1A**, Step 4, **Fig S1B**). The field was generated by a corona treater (Electro-Technic Products), the tip of which was moved around the PCR film for ~10 seconds. Without application of the electric field or undue physical force, spontaneous merging of droplets was rare (detected as incorrectly loaded microwells in **Fig S1B**). The kChip was imaged subsequently to measure the yield of the labeled strain, defined as the GFP signal at 0, 24, and 72 hr (**Fig 1A**, Step 5, **fig S1B-C**). We interpreted GFP signal as an indication of cell density of the labeled strain, as described previously (*33*, *34*).

Of the 22 kChips that were loaded well, two were removed downstream at the data analysis stage due to low GFP signal of the labeled strain (and cocultures containing these strains' unlabeled versions across the other kChips were also removed from the data analysis). We previously showed there is minimal evaporation in droplets between 24 and 72 hrs (*33*), and expect this has little effect on microbe growth given our observation that different microbes reach saturation in droplets and 96-well plate cultures on similar timescales.

We developed an image analysis pipeline, previously described (*33*) to: (a) Identify droplets as circular objects within the image; (b) Decode the contents of each droplet based on the color code; (c) Assign each droplet to a microwell; (d) filter out poorly loaded microwells from the data; and (e) Measure the average fluorescence of the merged droplets in each microwell.

Across the 20 kChips included in the data analysis, a total of 16,000 unique labeled/unlabeled/environment combinations were possible ([20 monocultures + (190 $\times$ 2) cocultures] $\times$ 40 environments = 16,000 combinations) (**Fig 1B**). After quality filtering data through our image analysis pipeline, the dataset contained 180,408 data points, with each of these combinations appearing 10.3 times on average and 97% appearing ≥3 times (**fig S4**). By integrating data among kChips, bidirectional pairwise interactions were deduced (**Fig 1C, fig S5, S6**).

We previously have shown that bacteria grow on kChip with growth dynamics similar to standard culture platforms like Erlenmeyer flasks and microtiter plates (*33*, *34*). We also expect the environment to be oxic throughout the time course of this experiment based on previous modeling of oxygen availability in droplets on kChip (though we have not measured this directly) (*33*, *34*). We note that the maturation of fluorescent GFP maturation in droplets, which can only occur in the presence of oxygen, as additional evidence of this oxic environment.

Fluorescence imaging

All fluorescence microscopy was performed using a Nikon Ti-E inverted fluorescence microscope with fluorescence excitation by a Lumencor Sola light emitting diode illuminator

(100% power setting). Images were taken across four fluorescence channels—three for the color codes and one additional channel for fluorescence-based assays. Each dye and the assay signal was detected with a different excitation wavelength generated by a collection of excitation filters: GFP by Semrock GFP-1828A (blue excitation); Alexa Fluor 555 dye by Semrock SpGold-B (green excitation); Alexa Fluor 594 dye by Semrock FF03-575/25-25 [excitation filter] + FF01-615/24-25 [emission filter] (yellow excitation); and Alexa Fluor 647 dye by Semrock LF635-B (red excitation). The emission signals corresponding to each dye channel were used to identify the contents of a given droplet within each droplet grouping prior to droplet merging (**Fig 3B)**. The final channel was used post-merge and at subsequent time points to quantify the assay signal (**Fig 3B)**. The camera possessed 16-bit depth (total pixel intensity range of 0-65,535 counts). Exposure times were chosen such that all assay signals and dye signals did not saturate (<20,000 counts).

Validation experiment in microtiter plates

To validate the interactions measured on the kChip, we cultured in 96-well plates all possible monocultures and cocultures from 7 bacterial strains in 4 different carbon sources. The resulting 84 conditions represent ~2% of the conditions measured on kChip. Each coculture condition in this follow-up experiment was grown in triplicate, and each monoculture in six replicates. The bacterial strains (RP1, KA, PAg2, LA, PP, PR2, PK, and a No-Strain control) were selected to cover a wide range of resource utilization profiles (**fig S2**), and the carbon sources (Uridine, Proline, Sucrose, Fumarate, and a No-Carbon control) were selected to cover a wide range of bidirectional interaction types (**fig 3A**).

The labeled and unlabeled bacterial strains were grown in monoculture in a starter phase (rich medium) and preculture phase (minimal medium) as described above. After washing the precultures with carbon-less M9 medium, and normalizing to a starting OD_{600} of 0.44 (22X), we mixed the labeled vs unlabeled bacteria in a matrix-like format in a 96-deepwell plate (100 µL each, 11X concentration each). Extra replicates of monocultures and intra-strain cocultures were added to the remaining columns of the same 96-deepwell plate. The four carbon sources were prepared in M9 media as described above, but to a concentration of 0.55% w/v. The experiment was initialized by mixing in triplicates (black-walled 96-well plates, Invitrogen) 136.4 µl of carbon source and 13.6 µl of bacterial mix (bringing the carbon and bacterial concentration to 0.5% w/v and 1X OD_{600} = 0.02, respectively). The plates were covered with gas-permeable AeraSeal membranes, and incubated for 72 hrs with shaking (220 rpm) and at room temperature (22-25ºC). Measurements of OD_{600} and GFP (ex. 480, em. 515, Optimal Gain, Z-Pos. 20 mm) were taken at 0, 24, 48, and 72hrs with a microplate reader (Infinite 200 Pro, Tecan). Before the 72hr time point, each well in the plates was mixed 20 times with a liquid handler (Viaflo 96, Integra) to break up accumulated biofilms. After the 72hr time point, one plate-replicate of Proline and Sucrose were serially diluted, and the dilutions 10^{-4}, 10^{-5}, and 10^{-6} were plated onto Nutrient Agar (3g yeast extract, 5g peptone, and 15g agar, Bacto, in one liter of water) with and without 15mg/L Chloramphenicol (plasmid pMRE132 confers resistance). The agar plates were incubated at room temperature for two days, and then the colonies were counted with the aid of a stereo microscope (Leica MZ10 F).

The OD600 values were normalized by subtracting the media-only control. The GFP values were normalized by dividing by the value of the media-only control from the corresponding time point, since each time point was measured using a different optical gain. Monoculture fold-growth calculated using GFP and OD600 values strongly agreed (**fig S8A**), indicating that bacterial growth can be well-quantified using GFP measurements. To compare the monoculture fold-growth in 96-well plates and on the kChip (**fig S8B**), the kChip GFP signal of each bacterial strain was

normalized by subtracting the 0.2 percentile signal at 0hrs. This subtraction corrects for the background fluorescence of the kChip wells with zero or very few cells (~580 arbitrary units of fluorescence), allowing for an estimation of the GFP signal at 0hr due to cells. To calculate the bacterial pairwise effects with GFP data from 96-well plates (**fig S8C-D**), we utilized the same formula and made the same background normalization as before (**fig S5, S6**), accounting for the inoculum effects on a per-replicate basis and for possible growth on media without carbon. For the Detection Limit (DL) in GFP measurements, we utilized the mean yield of strain A in coculture with strain B with no carbon source. No DL or background subtraction was used for the calculation of effects based on colony counts. Bidirectional interaction (**fig S8E**) types (Θ) and magnitudes (m) were calculated from the corresponding unidirectional interactions as described for the kChip measurements (**Fig 1F, fig S6**).

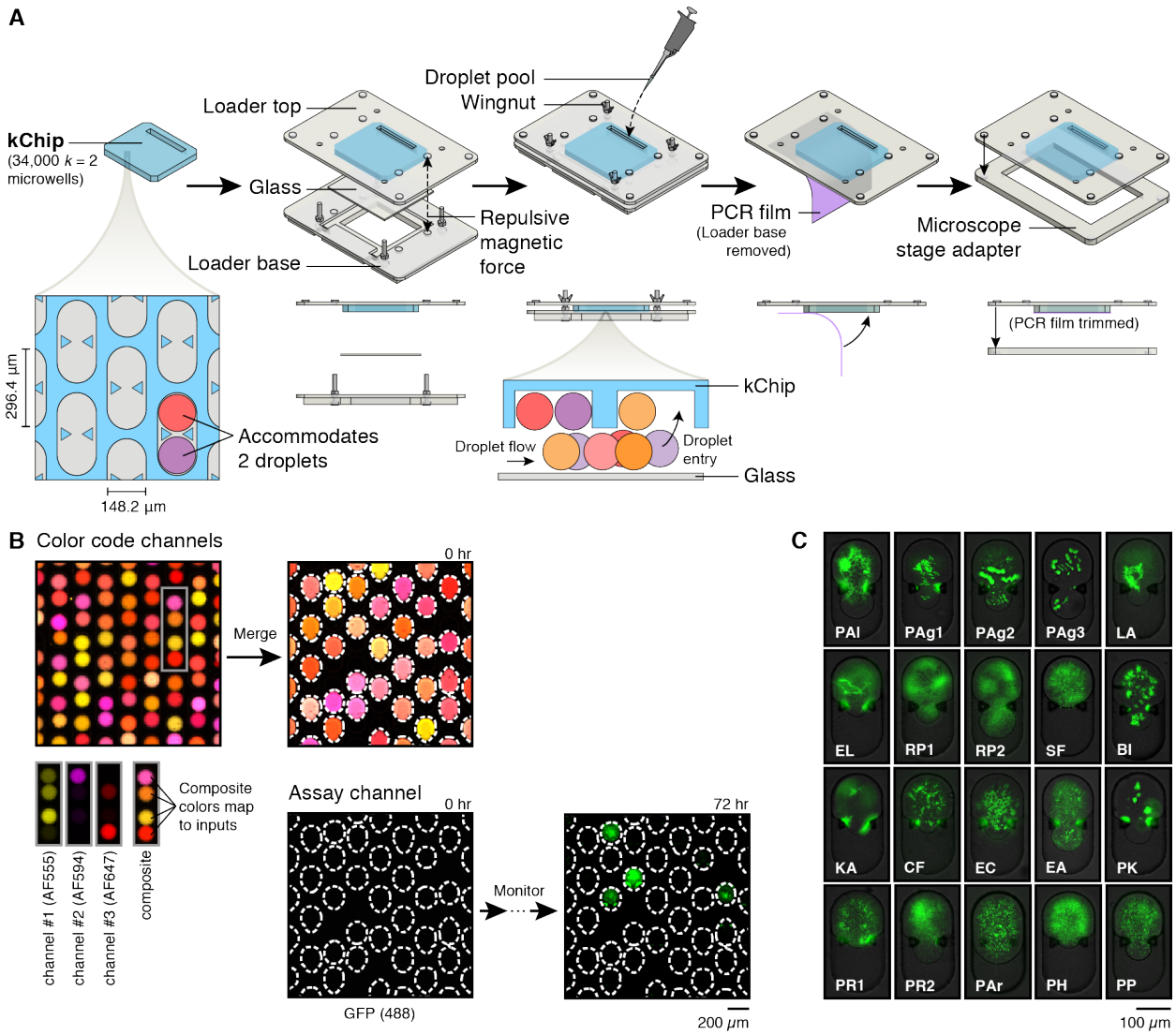

Fig S1. kChip experimental workflow. A. A kChip is chosen with a desirable microwell array layout, e.g. all $k = 2$ microwell geometries designed to capture two droplets each. Positioned inside of an acrylic loading apparatus, the kChip is suspended via repulsive magnetic interactions over a glass substrate to create a droplet flow space. Droplets are pipetted into a loading slot and enter microwells as they move through. After loading droplets, the kChip is sealed with a PCR film. **B.** The kChip is initially imaged in multiple channels (2X magnification) to determine the identity of each droplet. Here a specific ratio of three Alexa Fluor fluorescent dyes (AF555, AF594, and AF647) is used to barcode each droplet; the composite color indicates the droplet identity. After merging the droplets, an additional assay channel is used, e.g. GFP, to measure growth over time. **C.** Images of labeled strains in example cocultures (with arbitrary unlabeled strain and carbon source) (10X magnification). Full strain names are provided in **Table S1**.

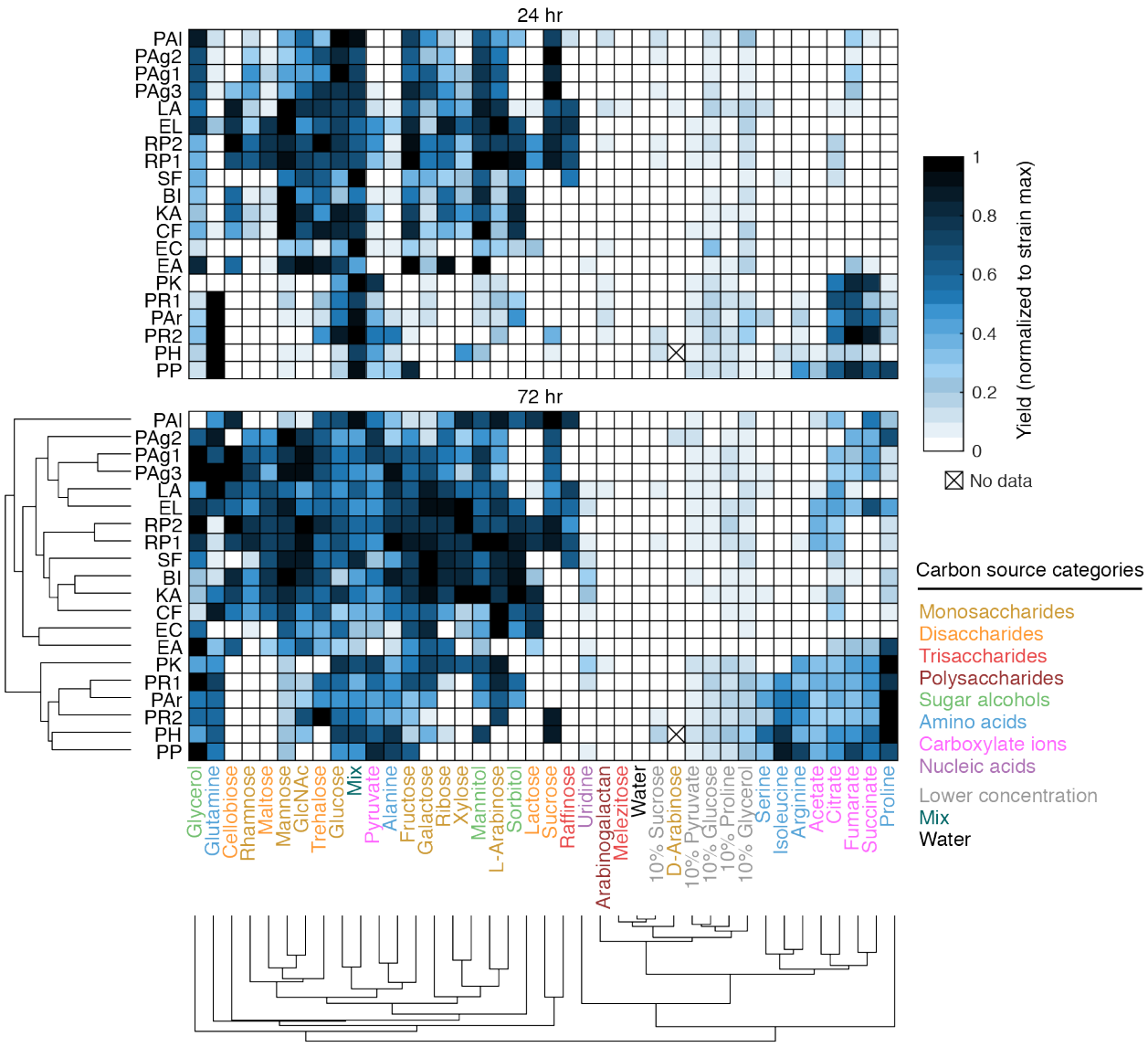

Fig S2. Carbon source utilization profiles of soil bacterial strains. Each strain's ability to grow on each carbon source was determined from kChip microwells containing a labeled strain in monoculture and a carbon source. Yield values (median GFP measurement across replicates) were background-subtracted (background = median yield of labeled strain with no carbon) and normalized to the maximum yield value observed (per strain per time point). Carbon sources and strains were hierarchically clustered at the 72 hr time point.

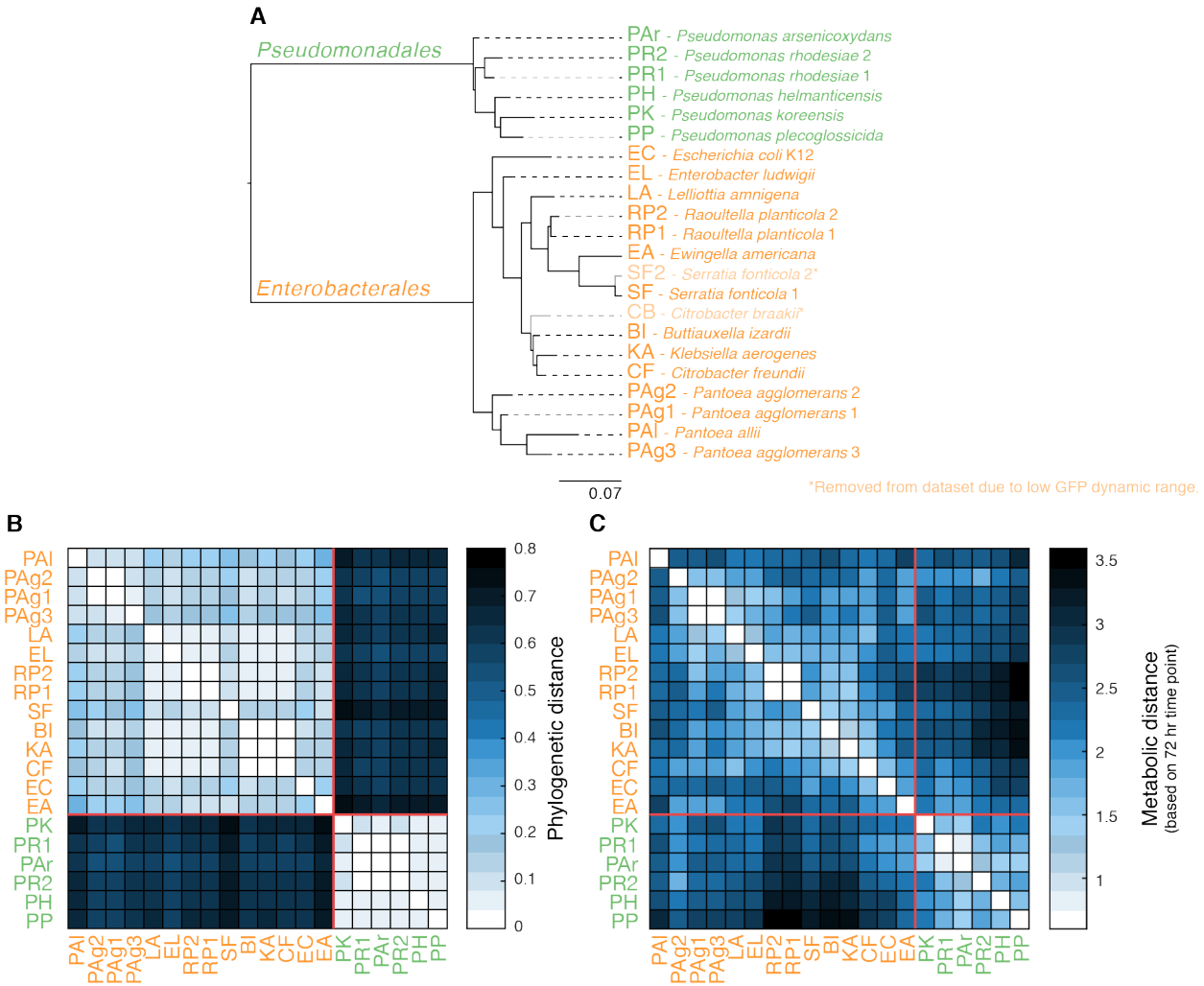

Fig S3. Strain pairwise comparison metrics. A. Phylogenetic tree built with maximum likelihood estimate, utilizing alignment of full 16S sequences. Sequences of the full 16S rRNA gene (~1500bp) were obtained via sanger sequencing. Sequences were trimmed to quality threshold ≥ 20 before merging the forward and reverse reads of each bacterial 16S. The sequence for *E. coli* K12 was obtained directly from NCBI. *Sulfolobus solfataricus*, a thermophilic archaeon, was used in the phylogenetic reconstruction as an outgroup species to root the tree. MUSCLE with default parameters was used to align the sequences. PhyML-SMS with default parameters was used to select GTR+G+I as the best model and to infer the tree. Units are 'Substitutions per base pair of the 16S gene. **B.** Pairwise phylogenetic distances between strains were calculated directly from the phylogenetic tree with R (Library Phytools, command 'drop.tip'). **C.** Metabolic distances ordered by carbon source utilization similarity. These distances were calculated as the Euclidean distance between two carbon source utilization profiles (**fig S2**). Red line = separation of two

taxonomic families. Orange font = strains of the order *Enterobacterales*. Green font = strains of the order *Pseudomonadales*.

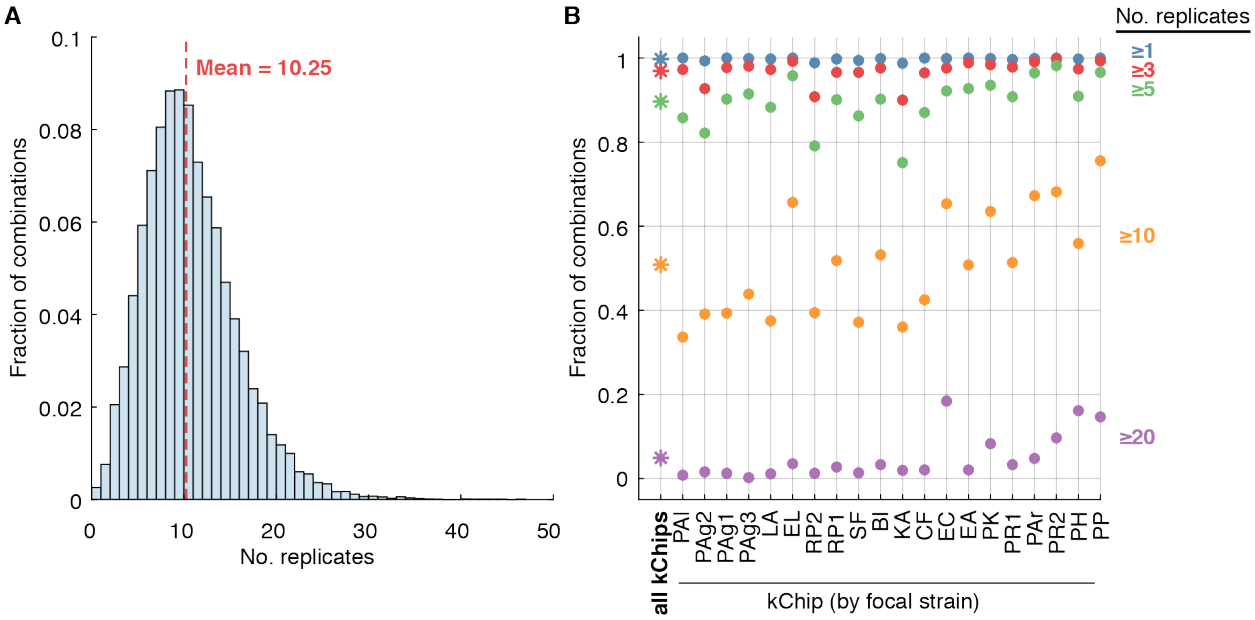

Fig S4. Combination sampling. A. Distribution of the number of replicates for all possible combinations of labeled strain/unlabeled strain/environment, including all 180,408 data points and representing all 17,600 possible combinations (i.e. all combinations of 20 labeled strains, [20 + 2

control] unlabeled strains, and [39 + 1 control] carbon sources). **B.** Fraction of combinations represented at least 1, 3, 5, 10, and 20 times for the entire dataset and per kChip.

A

$$E_{B \to A} = \text{Effect of unlabeled B on focal A} = \log_2 \frac{\max(A_{+B}, DL)}{\max(A_{mono}, DL)}$$

A_{+B} = background-subtracted median yield of focal A in coculture with B with given carbon source

A_{mono} = background-subtracted median yield of focal A in monoculture with given carbon source

DL = background-subtracted 90th percentile of A in coculture with B with no carbon source

B

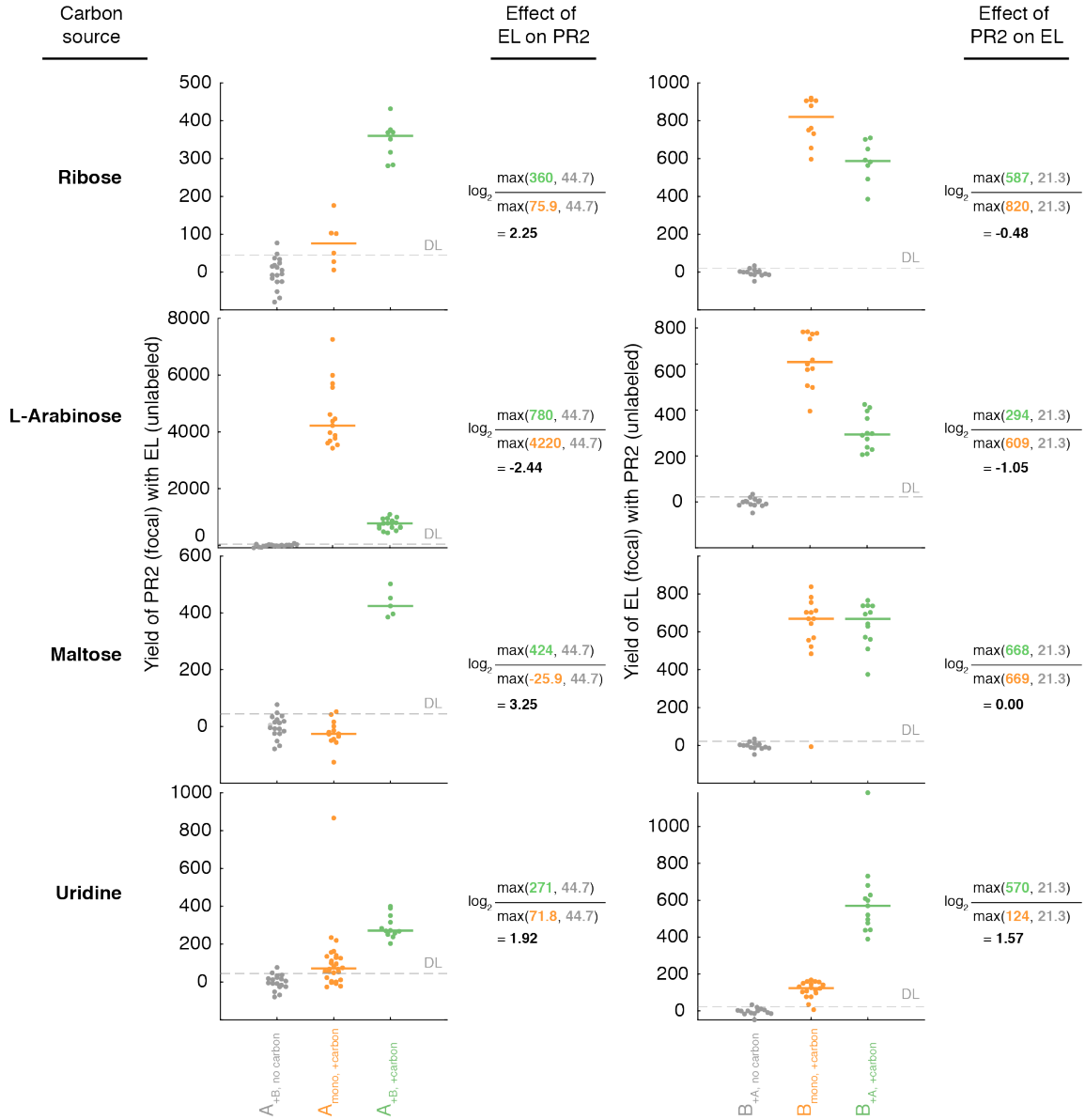

Fig S5. Interaction effect calculation. A. Formula for calculating effect of unlabeled strain B on yield of labeled strain A. **B.** Effect calculations for example coculture [*Enterobacter ludwigii* (EL) and *Pseudomonas rhodesiae* #2 (PR2)] on four example carbon sources.

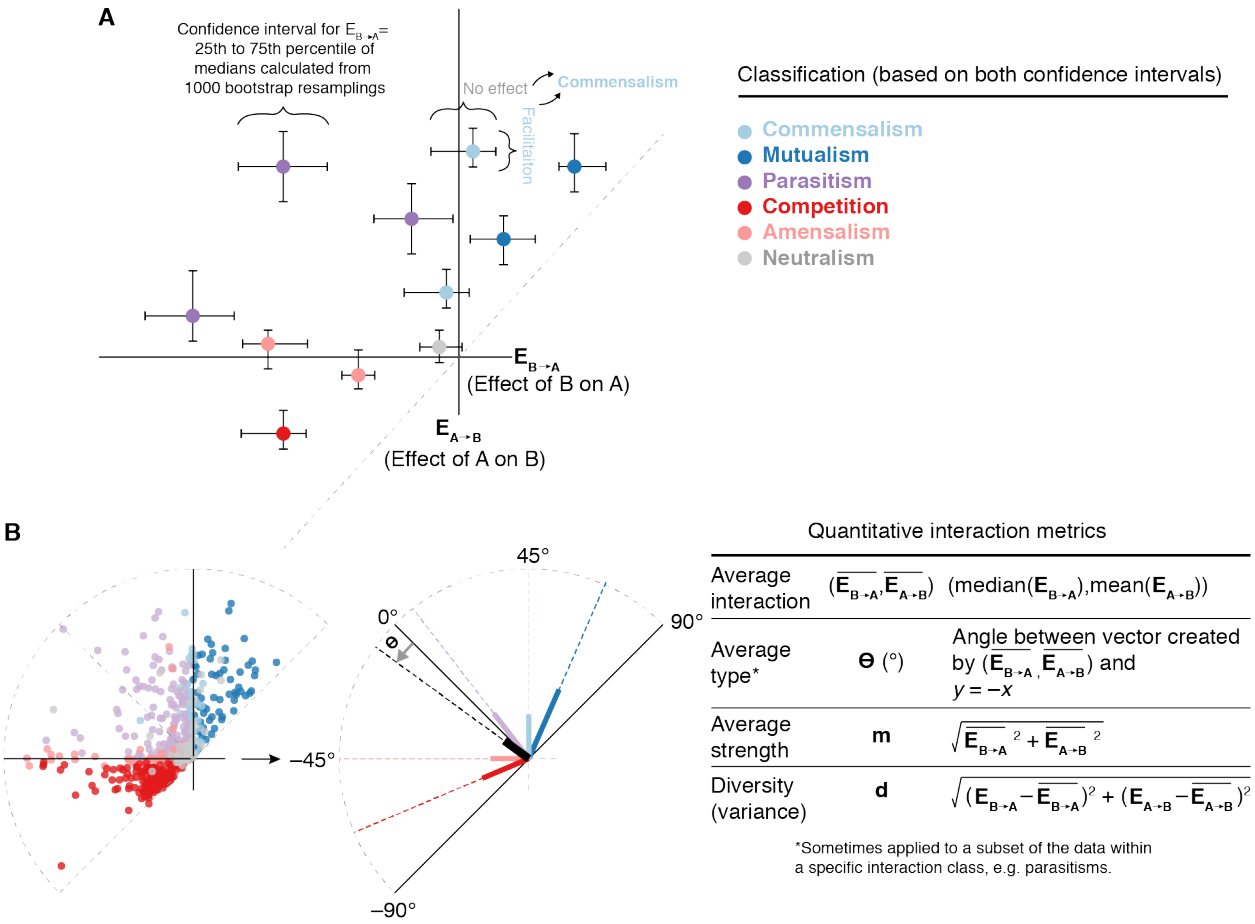

Fig S6. Pairwise interaction classification and quantitative metrics. A. Method for assigning pairwise interaction classification (commensalism, mutualism, parasitism, competition, amensalism, or neutralism). Confidence intervals for all one-way effects were generated by bootstrap resampling the effect calculation (**fig S5**). One-way interactions (facilitation, inhibition or no effect) were classified by the effect size and the fraction of the confidence interval that fell within the effect size's quadrant. Two-way interactions were classified by combining two one-way classifications. **B.** Quantitative metrics used to describe pairwise interactions. These include metrics for type, strength, and diversity (with diversity only applying to a set of interactions). The type metric was also used to subset of interactions belonging to specific interaction classifications.

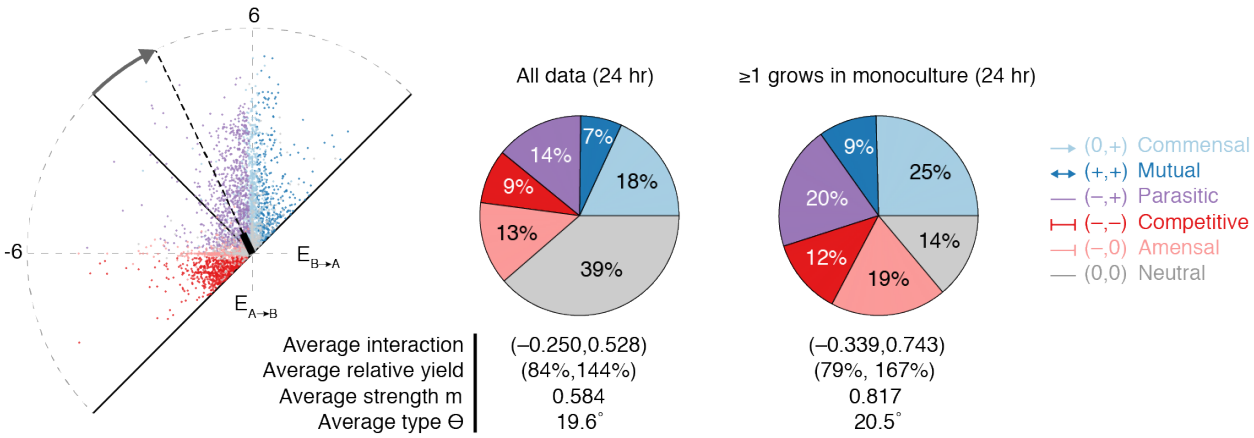

Fig S7. Interaction distributions for full dataset at 24 hr. (Left) All pairwise interactions at 24 hr on 33 distinct carbon sources. (Middle) Interaction classification of all data. (Right) Interaction classification excluding cases in which both strains comprising a coculture showed no detectable growth as monocultures on a given carbon source.

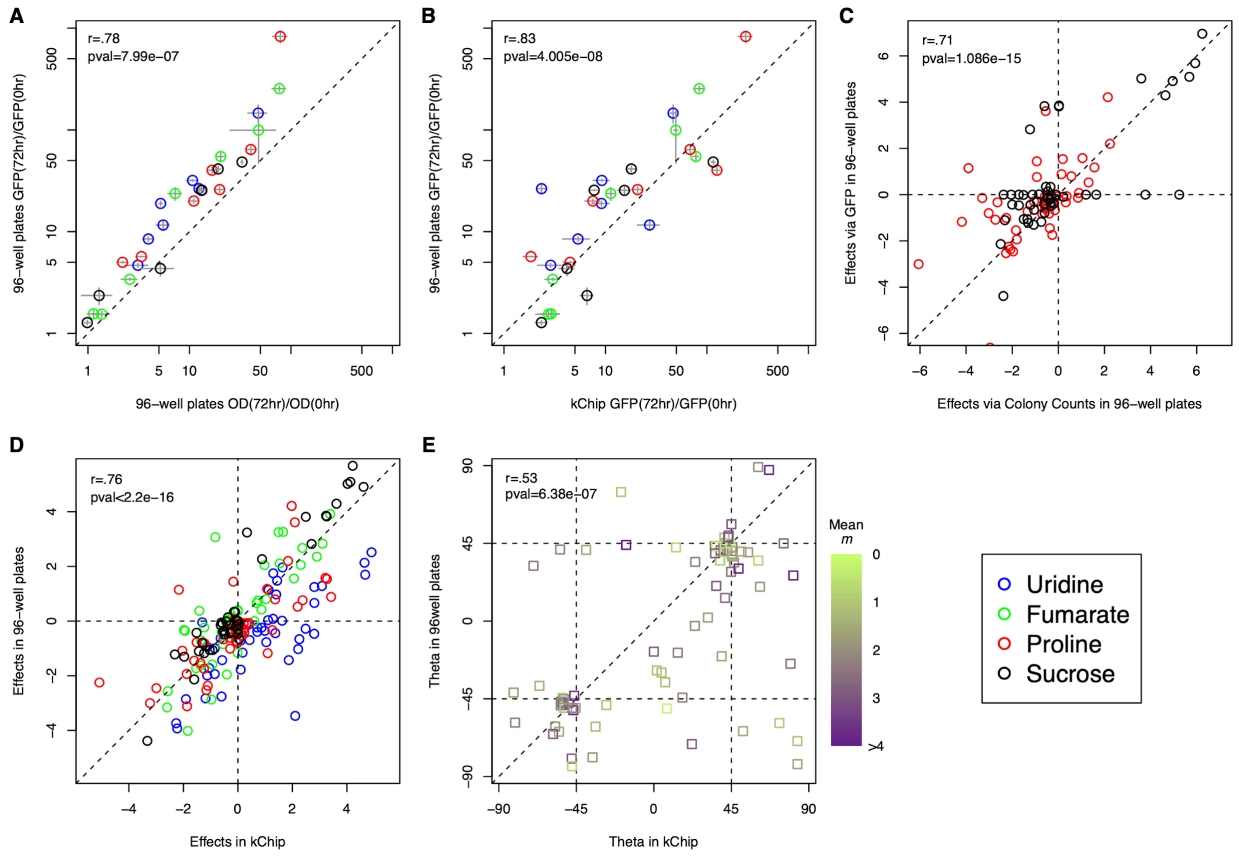

Fig. S8. Growth and interaction measurements in 96-well plates validate kChip measurements. A. Fold-growth of seven bacterial species in monoculture (RP1, KA, PAg2, LA, PP, PR2, and PK) calculated with optical density (OD600) and fluorescence intensity (GFP) in 96-well plates. Points are the mean of 6 replicates, and error bars are the standard error of the mean (s.e.m.). The colors denote the four different carbon sources (Uridine, Fumarate, Proline, and Sucrose). **B.** Monoculture fold-growth in 96-well plates and on kChip. kChip GFP yields were normalized by subtracting the 20th percentile yield at 0 hrs. **C.** Unidirectional pairwise effects among seven bacterial species in 96-well plates. The effects via colony counts and GFP measurements are calculated from two and three coculture replicates, respectively. **D.** Unidirectional effects calculated from GFP data from kChip and 96-well plates. **E.** Interaction type (Θ) calculated from kChip and 96-well plates data. The color of the points is the mean magnitude effect from both platforms. All Pearson correlation tests were calculated with a two-sided alternative hypothesis.

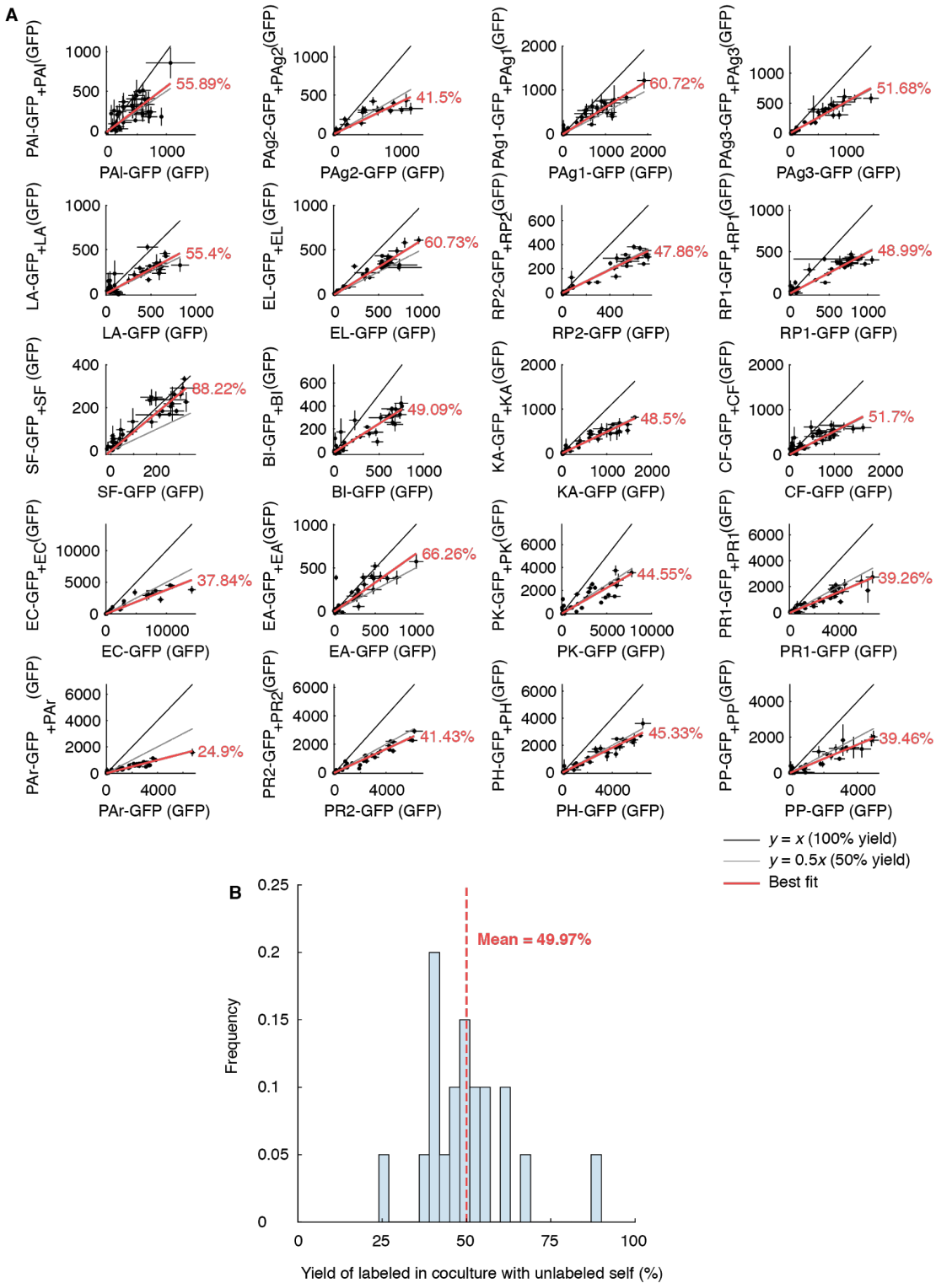

Fig S9. With-self interactions. A. Each plot represents an interaction between a labeled strain and its unlabeled counterpart on a given carbon source. *x*-axis = mean GFP of labeled strain when in monoculture; *y*-axis = mean GFP of labeled strain when cocultured with its unlabeled counterpart at a starting density of 1:1; each point = different carbon source; error bars = standard error of the respective mean values; red line = average fraction of the labeled strain relative to its monoculture

yield. **B.** Distribution of each strain's average growth with their respective unlabeled self-strains. All data at 72 hr.

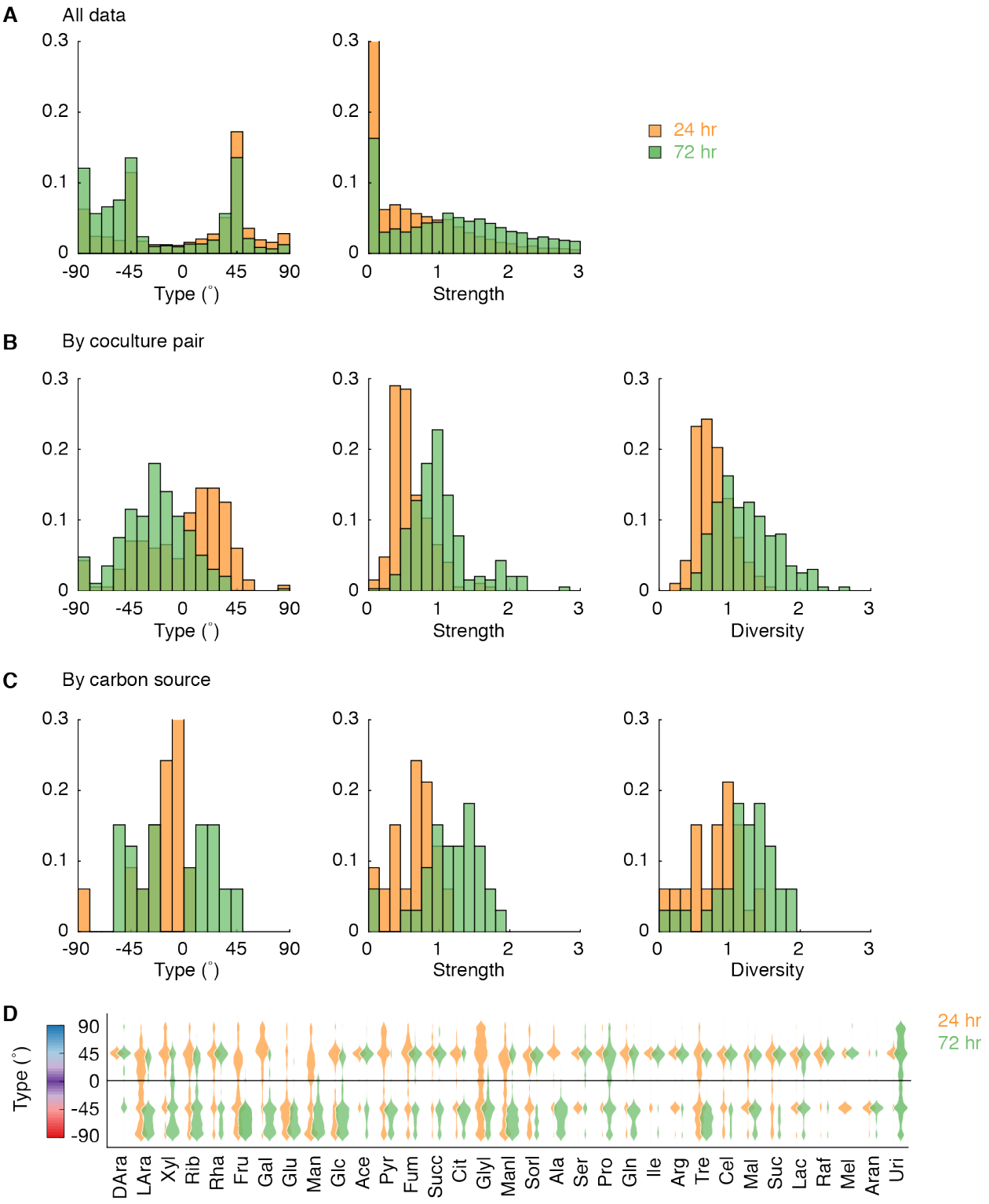

Fig S10. Interaction distributions by strain pair and by carbon source. A-C. Distributions of quantitative interaction metrics for all data (A), data averaged by strain pair (B), and data averaged by carbon source (C). Calculations for averages are described in **fig S6. D.** Distributions of interaction type metric organized by carbon source.

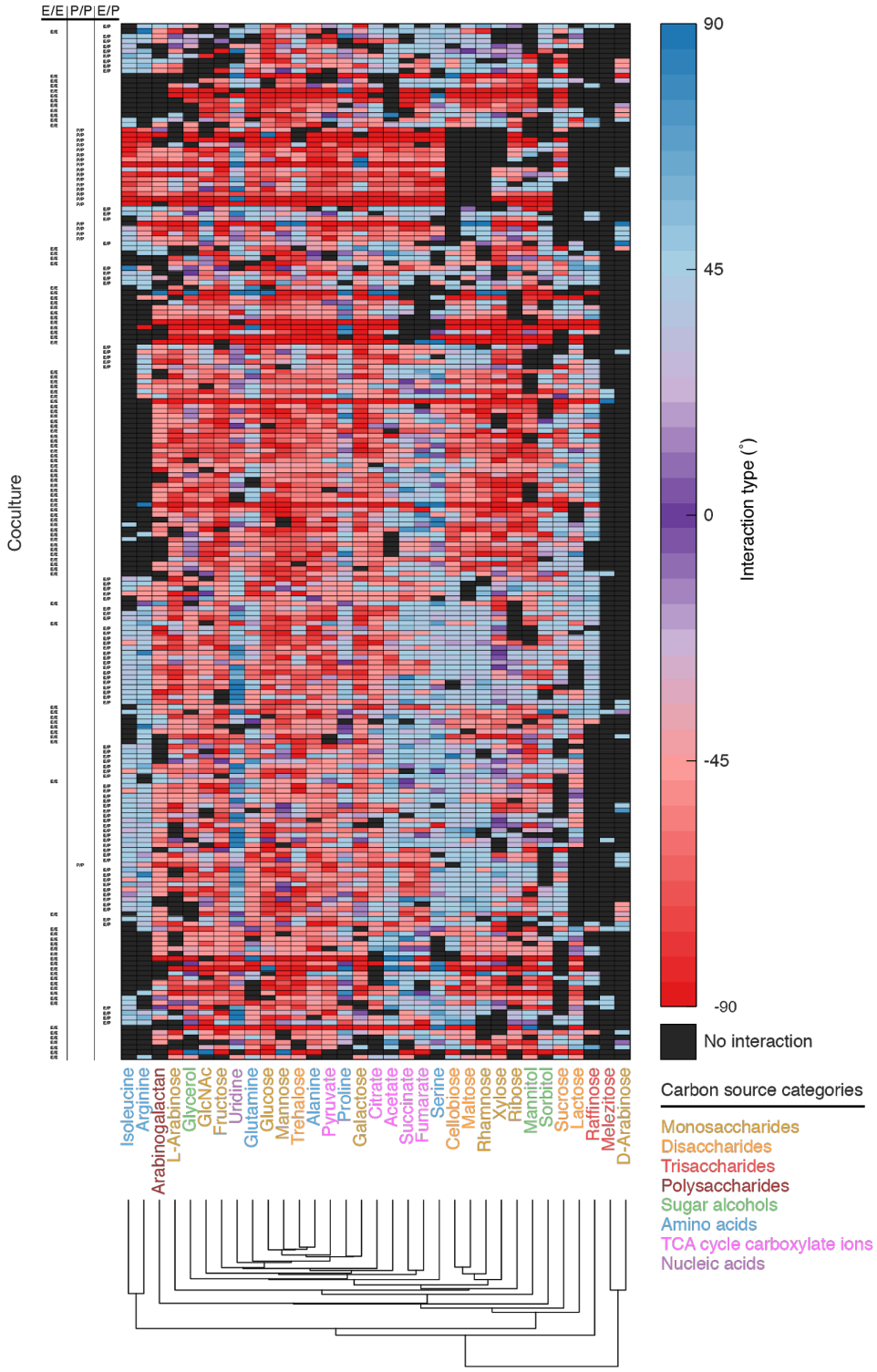

Fig S11. Interaction types for full dataset. Strain pairs and carbon sources were hierarchically clustered by interaction type. E = *Enterobacterales*. P = *Pseudomonadales*. All data at 72 hr.

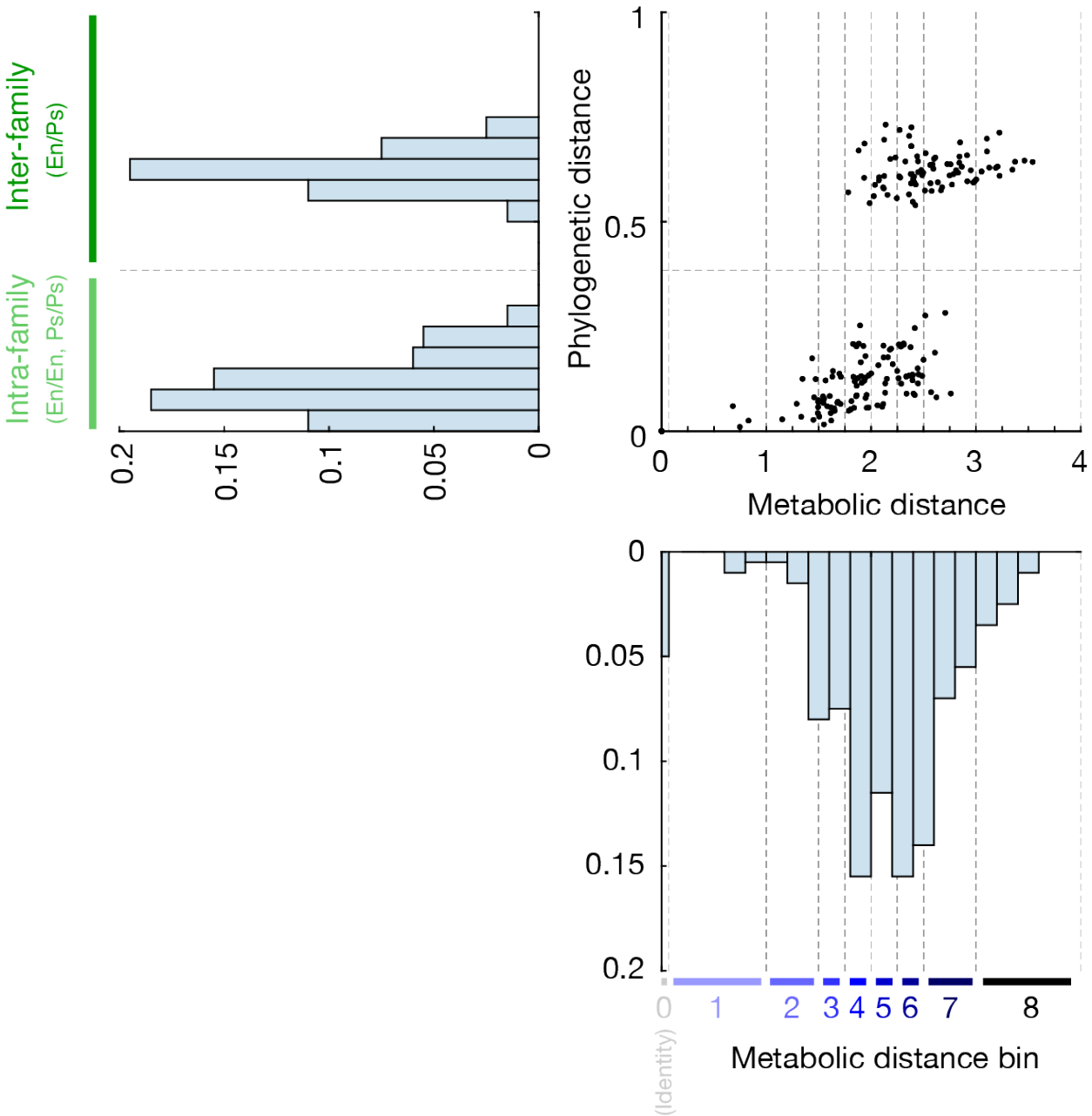

Fig S12. Binning of phylogenetic and metabolic distances. Phylogenetic distances occupied a bimodal distribution representing intra-family and inter-family pairs. Metabolic distances occupied a continuous distribution. Metabolic distances bins were drawn to capture roughly even numbers of pairs. In the dense center of the distribution, bins were evenly spaced by 0.25 metabolic distance units (Bins #3-6). The next outermost bins occupied 0.5 metabolic distance units (Bins #2 and #7), and the most outermost bins occupied 1 metabolic distance unit (Bins #1 and #8). Bin #0 represents with-self interactions (with a metabolic distance of 0). En = *Enterobacteriaceae*. Ps = *Pseudomonadaceae*.

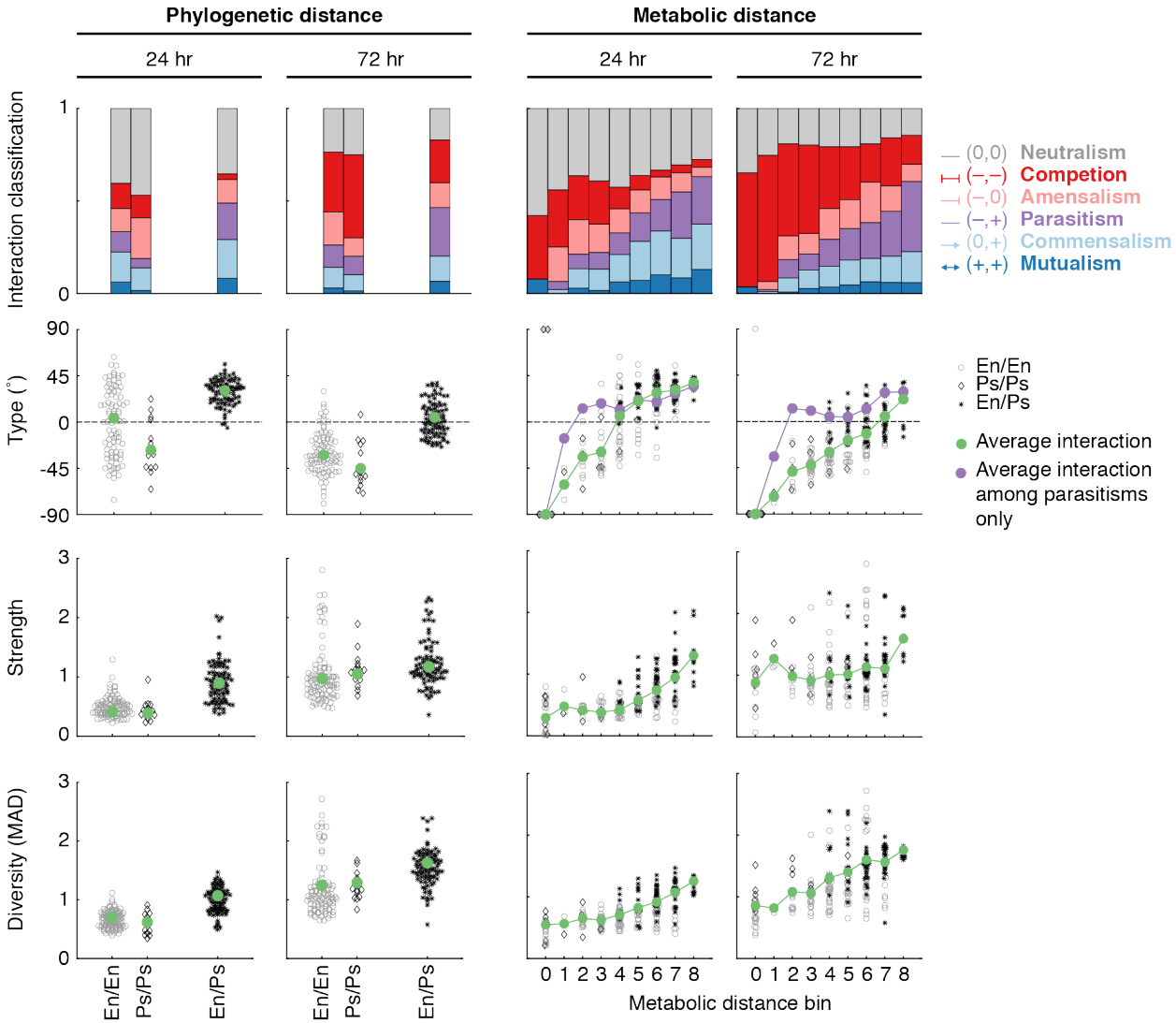

Fig S13. Interaction metrics by phylogenetic and metabolic distance bins. Phylogenetic bins represent the intra-family interactions (En/En and Ps/Ps) and inter-family interaction (En/Ps). Metabolic bins represent increasingly metabolically different pairs and are described in **fig S12**.

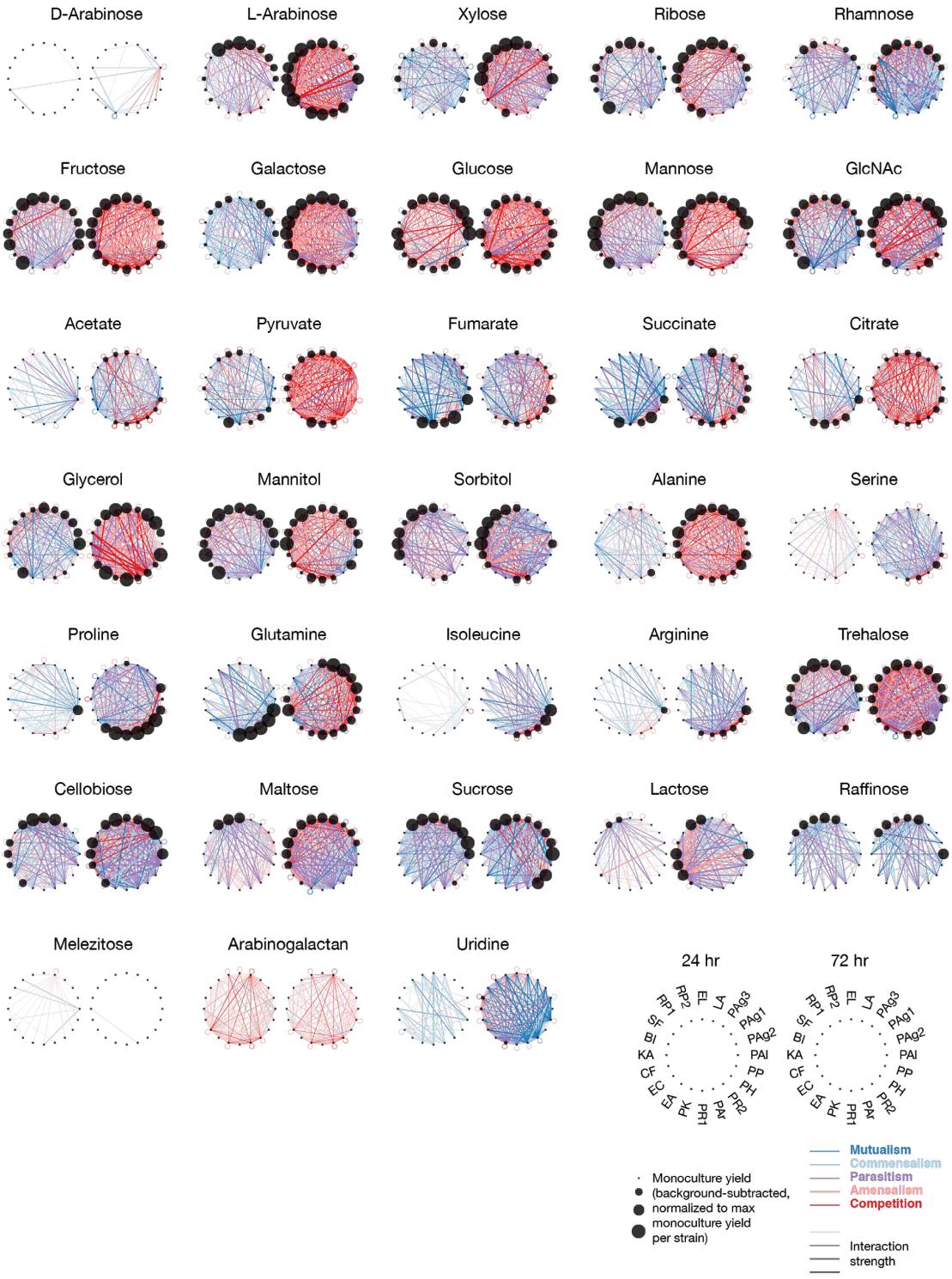

Fig S14. Interaction networks for each carbon source. For each carbon source, the pairwise interaction network is plotted at 24 hr (left) and 72 hr (right). The legend (bottom-right) indicates the strain identity of each node. Node size represents monoculture yield (background-subtracted and normalized to maximum monoculture yield per strain). Edge color represents interaction classification. Edge thickness represents interaction strength.

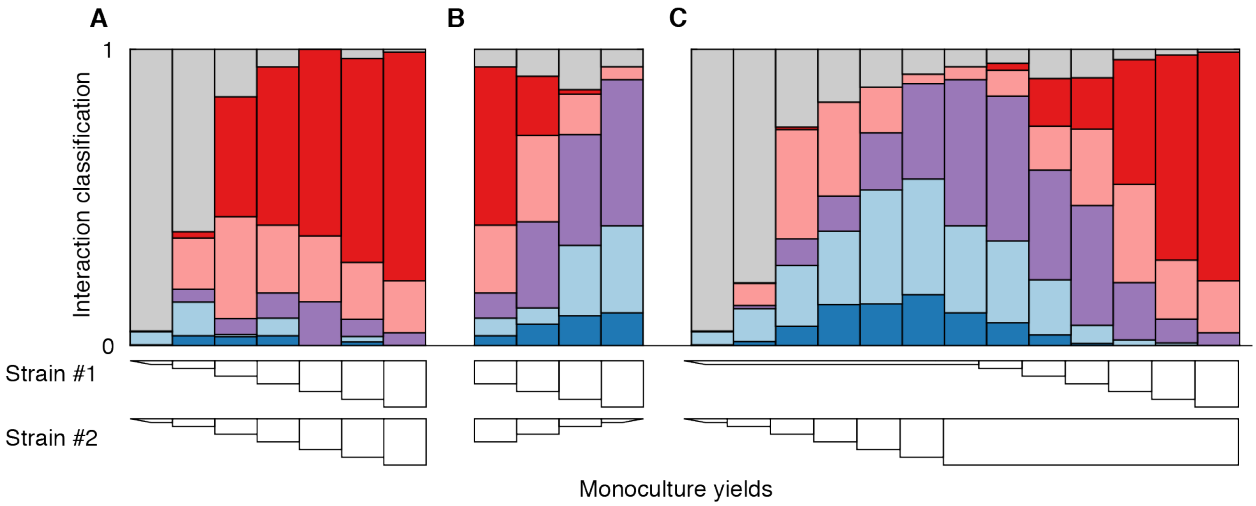

Fig S15. Interaction classification by monoculture yield comparisons. Interaction classification when both strains are increasing in monoculture yield across carbon sources (**A**), one strain is increasing and the other is decreasing in monoculture yield (**B**), and one held constant at no-growth or maximum growth while the other strain is increasing in monoculture yield (**C**). Colors indicate interaction classification (with color legend in **Fig 2**). All data at 72 hr.

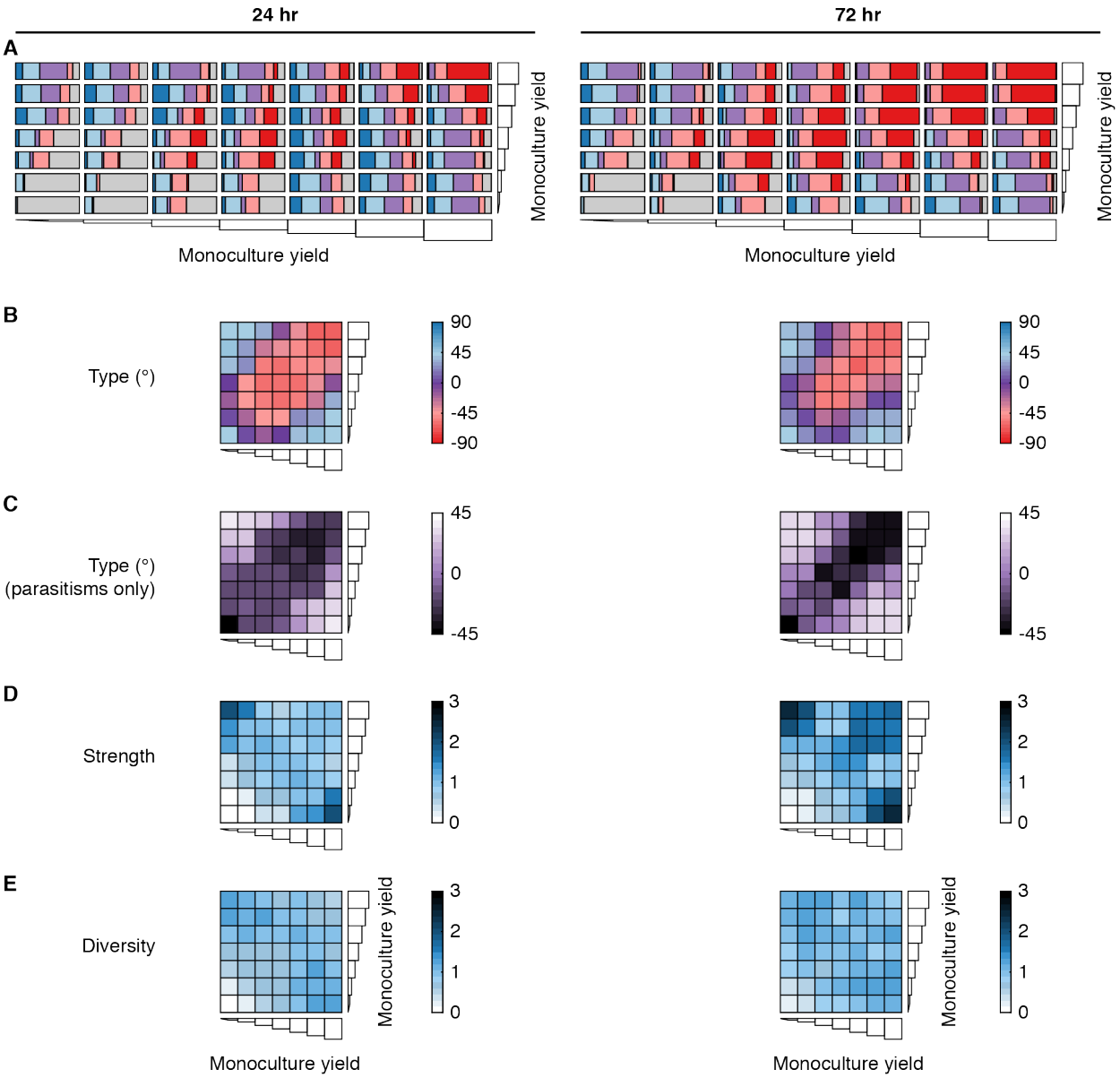

Fig S16. Interactions by monoculture yields. A. Interaction classification for all monoculture yield combinations. Monoculture yields were normalized based on monoculture yields at the given time point. Colors indicate interaction classification (with color legend in Fig 2). **B-D.** Average interaction metrics for all monoculture yield combinations.

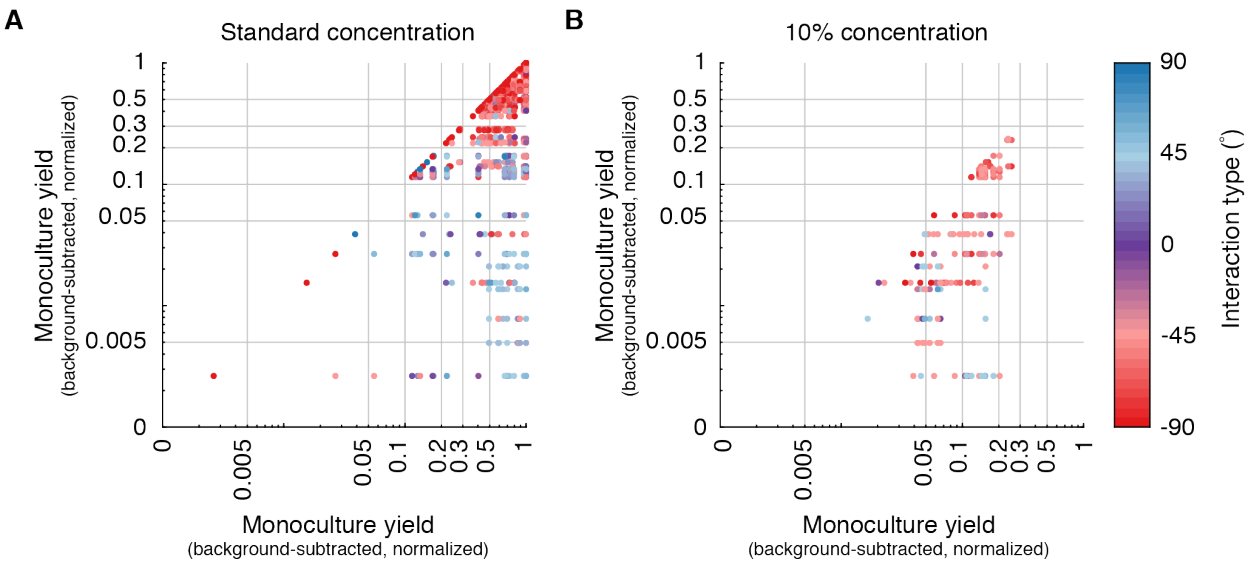

Fig S17. Interactions arranged by monoculture yields for standard and 10% concentration. At standard concentration (0.5% w/v) (left) and 10% concentration (0.05% w/v) (right) of carbon sources, monoculture yields and interactions were both different. All interactions at 72 hr.

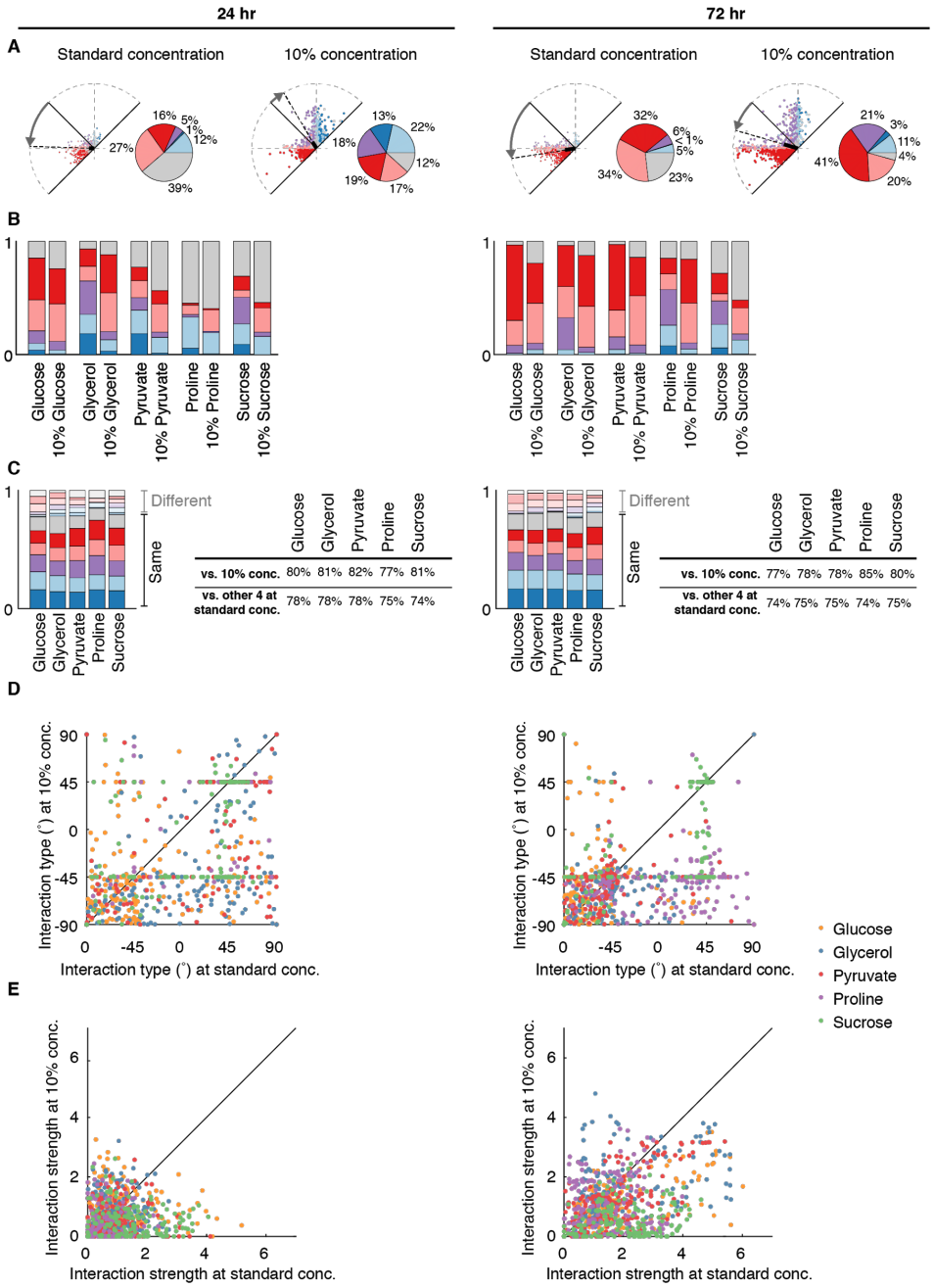

Fig S18. Interactions with carbon sources at lower concentration. A. All interactions occurring on 5 carbon sources (glucose, glycerol, pyruvate, proline, and sucrose) at standard concentration (0.5% w/v) and 10% concentration (0.05% w/v). **B.** Interaction classifications per carbon sources for standard and 10% concentrations. Colors indicate interaction classification (with color legend in Fig 2) **C.** Interaction classifications that are the same between the standard and 10% conditions (unmuted colors) and different (muted colors). The tables indicate the percentage agreement in interaction classification between the standard and 10% concentrations (first row) and the average percentage agreement with the 4 other carbon sources at standard concentration (second row). **D-E.** The interaction type and strength for all strain pairs at standard vs. 10% concentration, colored by carbon source.

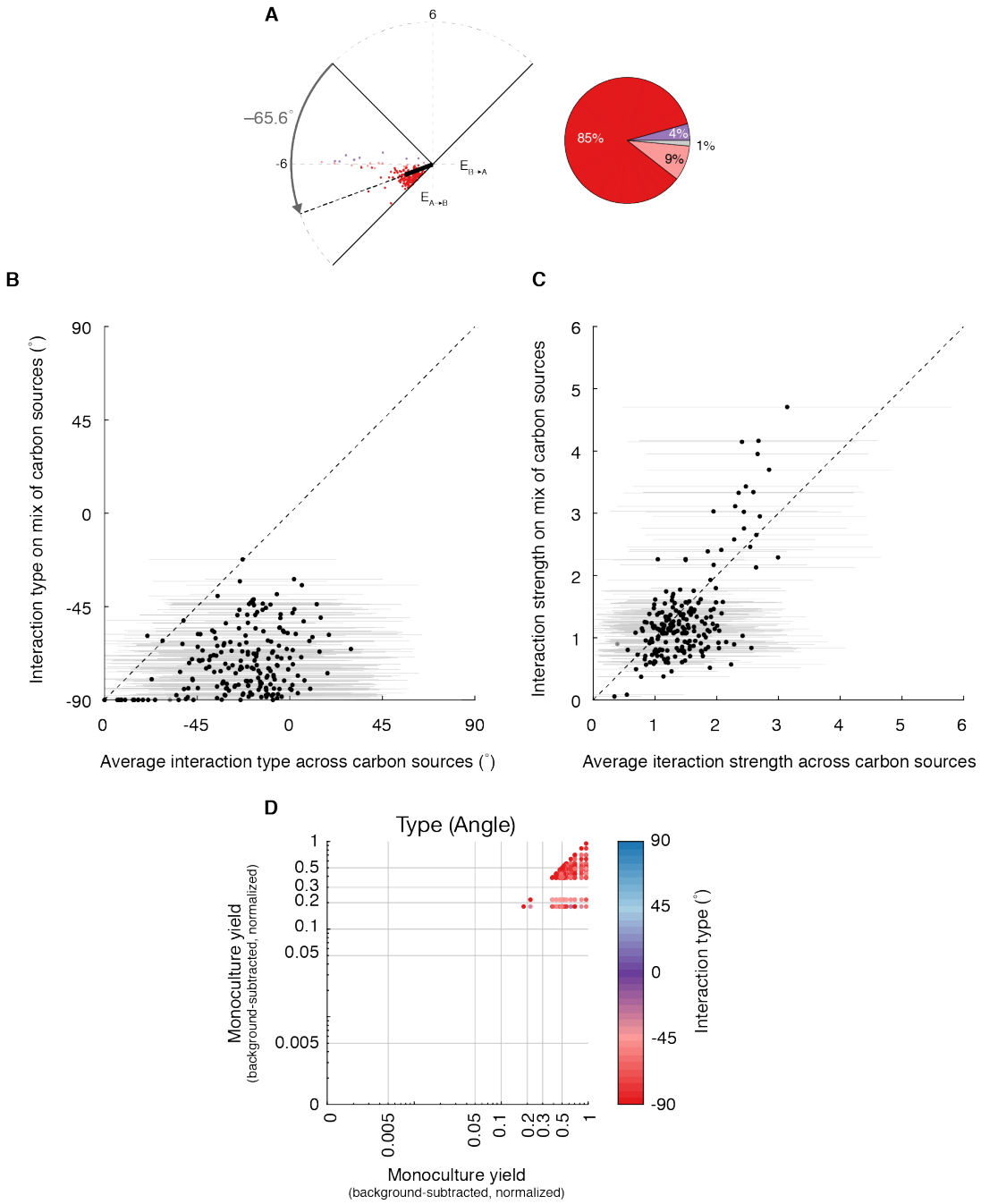

Fig S19. Interactions on a mix of carbon sources. A. All interactions on an even mix of 33 carbon sources (each at 0.015% w/v, total concentration 0.5% w/v). Colors indicate interaction classification (with color legend in Fig 2). **B.** Comparison of interaction type for each coculture on the mix of carbon sources and mean interaction type on all 33 single carbon sources. Error bars indicate standard deviation. **C.** Comparison of interaction strength for each coculture on the mix of carbon sources and mean interaction strength on all 33 single carbon sources. Error bars indicate standard deviation. **D.** Interactions arranged by monoculture yield. All interactions at 72 hr.

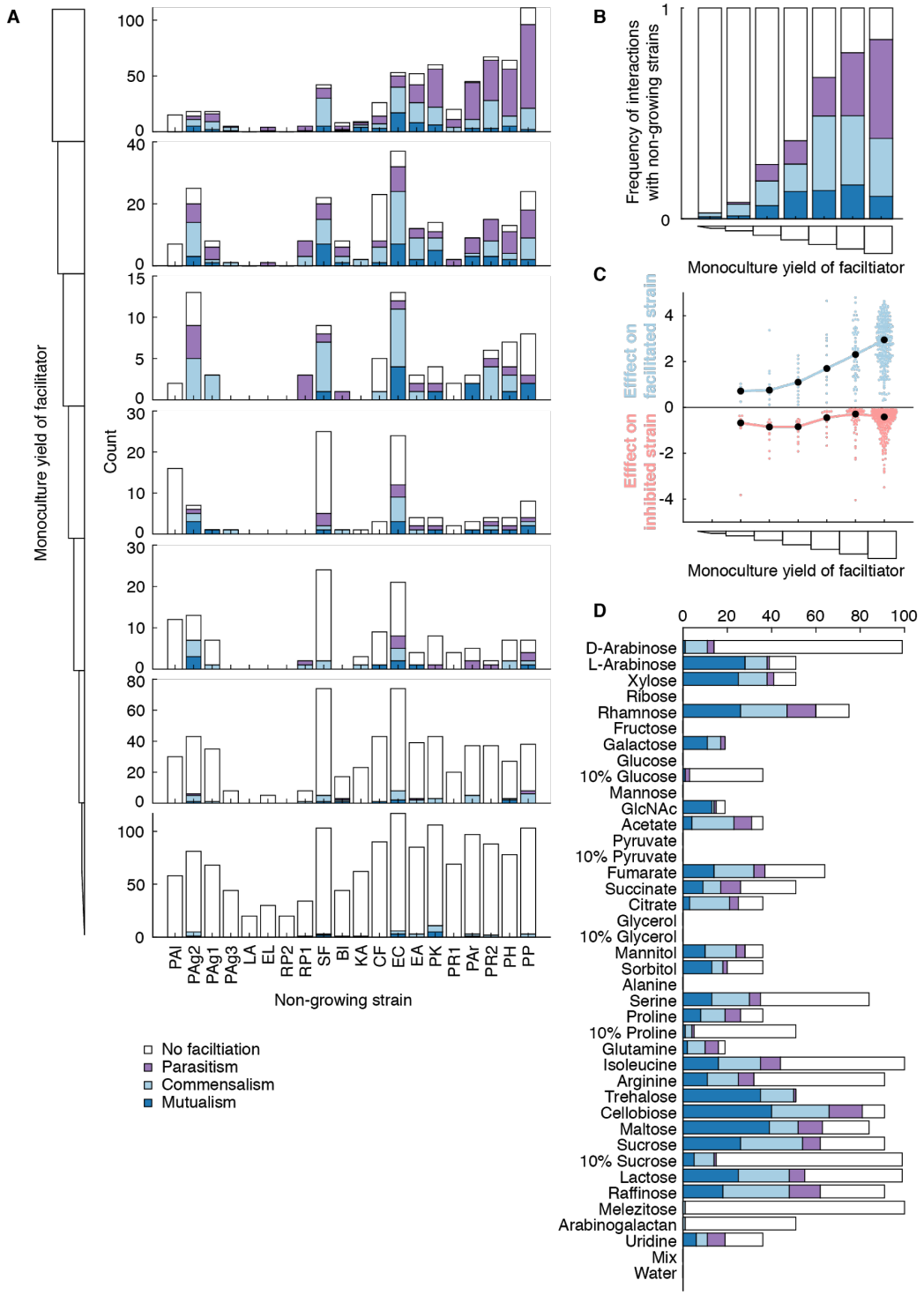

Fig S20. Interactions containing obligate facilitation. A. Interactions between growers and non-growers separated by monoculture yield of the facilitator. **B.** Each bar represents all interactions for each subplot in panel A (normalized to 1). **C.** Effect sizes for parasitisms where one strain was obligately facilitated. **D.** Interactions between growers and non-growers separated by carbon source.

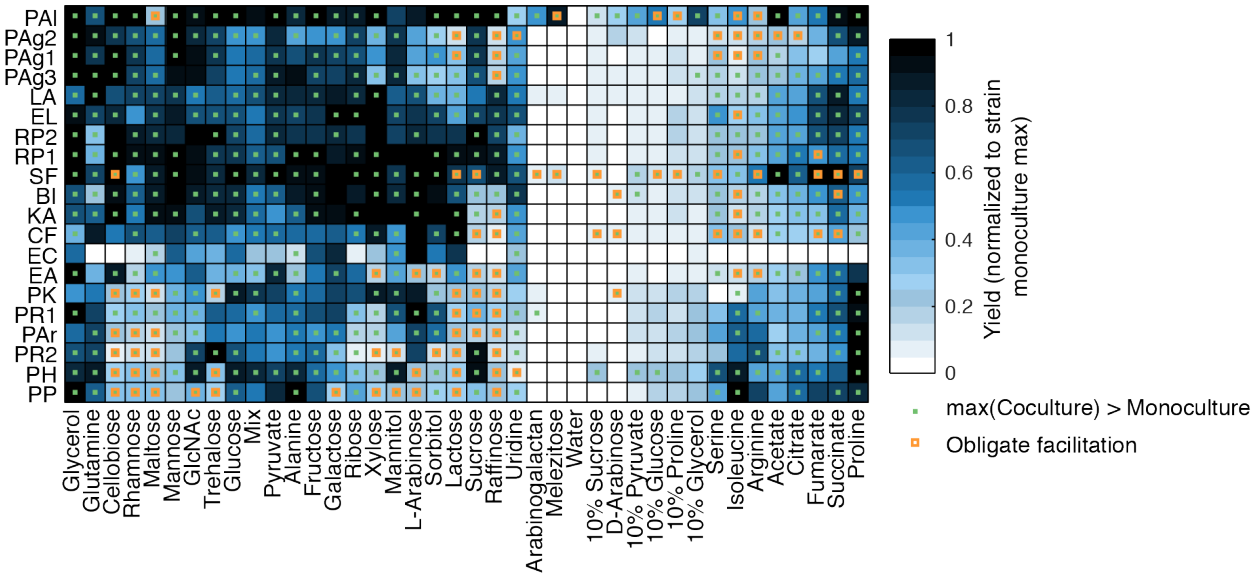

Fig S21. Maximum yields across all dataset. Yield values (median GFP measurement across replicates) were background-subtracted (background = median yield of labeled strain with no carbon) and normalized to the maximum yield value observed for the given strain in monoculture. Carbon sources and strains were hierarchically clustered at the 72 hr time point based on their monoculture yields only. Green dots indicate that the maximum yield of the strain/carbon source combination occurred in a coculture was at least 0.1 normalized units greater than the monoculture yield. Orange squares indicate obligate facilitation where the strain did not grow detectably on the carbon source. All interactions at 72 hr.

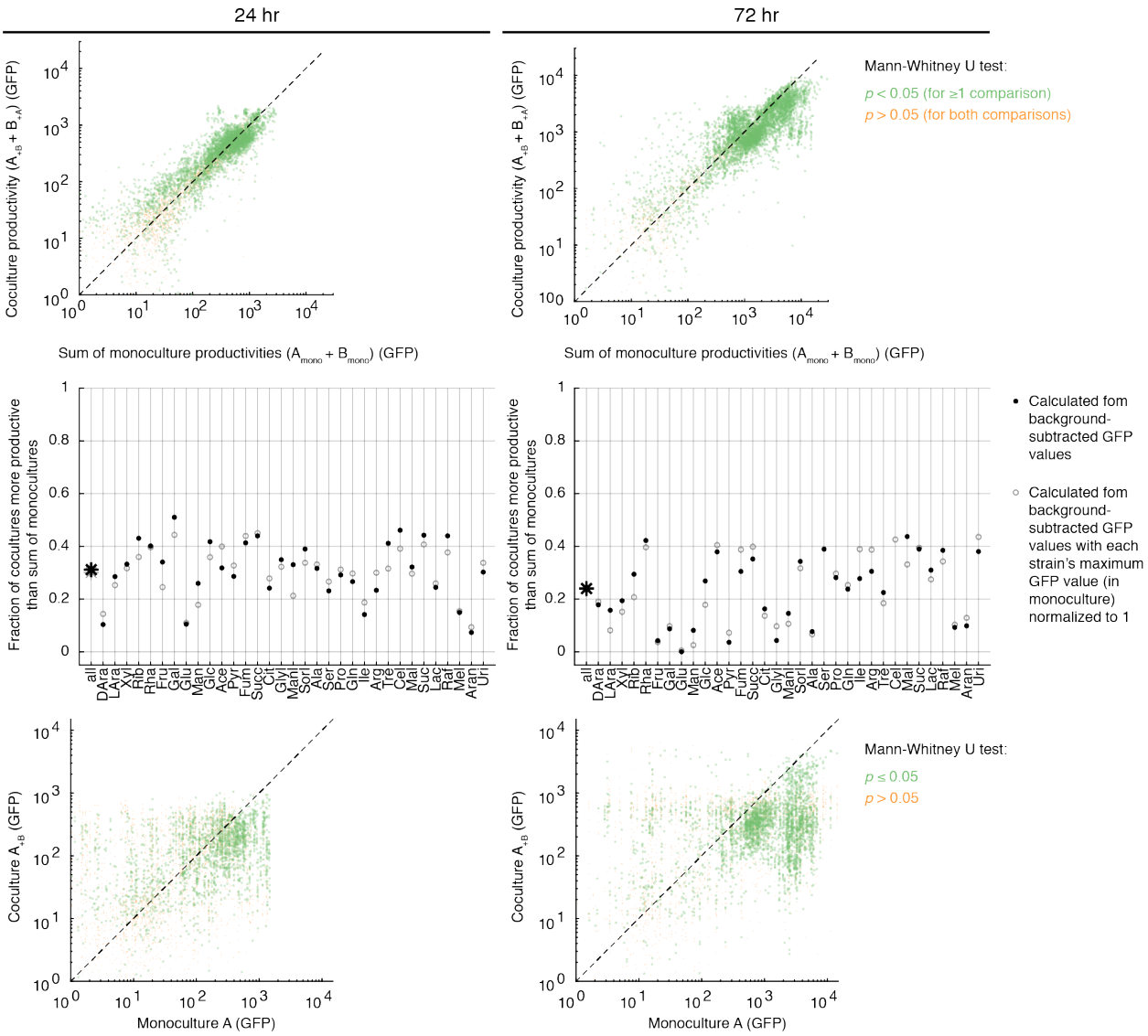

Fig S22. Coculture vs. monoculture comparison. (Top) Coculture productivity vs. sum of monoculture productivities. Each point represents a coculture/carbon source combination. The 33 0.5% w/v carbon sources are included. Yields calculated as background-subtracted GFP. (Middle) The fraction of cocultures more productive than the sum of monocultures for total dataset (star) and broken down by each carbon source. The solid black circles represent fractions calculated based on background-subtracted GFP values. The open gray circles represent values calculated based on background-subtracted GFP values that were then normalized to the maximum monoculture value for each strain (as in **Fig S2**). (Bottom) The yield in coculture vs. monoculture. Each point represents a coculture/carbon source combination. Yield calculated as background-subtracted GFP.

No.	Source	Order	Closest Seqmatch (16S Gene)	Strain shorthand
1	Middlesex Fells	*Enterobacterales*	*Ewingella americana*	EA
2	Middlesex Fells	*Enterobacterales*	*Raoultella planticola*	RP1
3	Middlesex Fells	*Enterobacterales*	*Buttiauxella izardii*	BI
4	Middlesex Fells	*Enterobacterales*	*Citrobacter freundii*	CF
5	Killian Court	*Enterobacterales*	*Pantoea agglomerans*	PAg1
6	Killian Court	*Enterobacterales*	*Klebsiella aerogenes*	KA
7	Killian Court	*Enterobacterales*	*Raoultella planticola*	RP2
8	Killian Court	*Enterobacterales*	*Pantoea agglomerans*	PAg2
9	Killian Court	*Enterobacterales*	*Serratia fonticola*	SF1
10	Killian Court	*Enterobacterales*	*Lelliottia amnigena*	LA
11	Killian Court	*Enterobacterales*	*Pantoea allii*	PAl
12	Killian Court	*Enterobacterales*	*Pantoea agglomerans*	PAg3
13	Harvard Yard	*Pseudomonadales*	*Pseudomonas helmanticensis*	PH
14	Lalicata Compost	*Pseudomonadales*	*Pseudomonas rhodesiae*	PR1
15	Tech Square Yard	*Pseudomonadales*	*Pseudomonas plecoglossicida*	PP
16	Office Plant	*Enterobacterales*	*Enterobacter ludwigii*	EL
17	Charles River Soil	*Pseudomonadales*	*Pseudomonas rhodesiae*	PR2
18	Charles River Soil	*Pseudomonadales*	*Pseudomonas koreensis*	PK
19	Harvard Yard	*Pseudomonadales*	*Pseudomonas arsenicoxydans*	PAr
20	Lab strain	*Enterobacterales*	*Escherichia coli*	EC

Table S1. Strains used in coculture experiment

No.	Biochemical class	Full compound	Name used	Abbrev.	% w/v of Compound	No. carbon atoms	Total molar mass (g)	Carbon component molar mass (g)	Molarity of carbon component (mol/L)
1	Monosaccharide	D-Arabinose	D-Arabinose	DAra	0.5	5	150.13	150.13	0.333
2	Monosaccharide	L-Arabinose	L-Arabinose	LAra	0.5	5	150.13	150.13	0.333
3	Monosaccharide	D-Xylose	Xylose	Xyl	0.5	5	150.13	150.13	0.333
4	Monosaccharide	D-Ribose	Ribose	Rib	0.5	5	150.13	150.13	0.333
5	Monosaccharide	L-Rhamnose monohydrate	Rhamnose	Rha	0.5	6	182.17	164.16	0.305
6	Monosaccharide	D-Fructose	Fructose	Fru	0.5	6	180.16	180.16	0.278
7	Monosaccharide	D-Galactose	Galactose	Gal	0.5	6	180.16	180.16	0.278
8	Monosaccharide	D-Glucose	Glucose	Glu	0.5	6	180.16	180.16	0.278
9	Low conc.	0.1X D-Glucose	Glucose01	Glu01	0.05	6	180.16	180.16	0.278
10	Monosaccharide	D-Mannose	Mannose	Man	0.5	6	180.16	180.16	0.278
11	Monosaccharide	N-Acetyl-D-glucosamine	GlcNAc	Glc	0.5	8	221.21	221.21	0.226
12	TCA	Sodium acetate	Acetate	Ace	0.5	2	82.03	59.04	0.847
13	TCA	Sodium pyruvate	Pyruvate	Pyr	0.5	3	110.04	87.05	0.574
14	Low conc.	0.1X Sodium pyruvate	Pyruvate01	Pyr01	0.5	3	110.04	87.05	0.574
15	TCA	Sodium fumarate dibasic	Fumarate	Fum	0.5	4	160.04	114.06	0.438
16	TCA	Disodium succinate	Succinate	Succ	0.5	4	162.05	116.07	0.431
17	TCA	Sodium citrate dihydrate	Citrate	Cit	0.5	6	294.1	189.1	0.264
18	Sugar alcohol	Glycerol	Glycerol	Glyl	0.5	3	92.09	92.09	0.543
19	Low conc.	0.1X Glycerol	Glycerol01	Glyl01	0.05	3	92.09	92.09	0.543
20	Sugar alcohol	D-Mannitol	Mannitol	Manl	0.5	6	182.17	182.17	0.274
21	Sugar alcohol	D-Sorbitol	Sorbitol	Sorl	0.5	6	182.17	182.17	0.274
22	Amino acid	L-Alanine	Alanine	Ala	0.5	3	89.09	89.09	0.561
23	Amino acid	L-Serine	Serine	Ser	0.5	3	105.09	105.09	0.476
24	Amino acid	L-Proline	Proline	Pro	0.5	5	115.13	115.13	0.434
25	Low conc.	0.1X L-Proline	Proline01	Pro01	0.05	5	115.13	115.13	0.434

26	Amino acid	L-Glutamine	Glutamine	Gln	0.5	5	146.14	146.14	0.342
27	Amino acid	L-Isoleucine	Isoleucine	Ile	0.5	6	131.17	131.17	0.381
28	Amino acid	L-Arginine	Arginine	Arg	0.5	6	174.2	174.2	0.287
29	Disaccharide	D-Trehalose dihydrate	Trehalose	Tre	0.5	12	378.33	342.3	0.146
30	Disaccharide	D-Cellobiose	Cellobiose	Cel	0.5	12	342.3	342.3	0.146
31	Disaccharide	D-Maltose monohydrate	Maltose	Mal	0.5	12	342.3	342.3	0.146
32	Disaccharide	D-Sucrose	Sucrose	Suc	0.5	12	342.3	342.3	0.146
33	Low conc.	0.1X D-Sucrose	Sucrose01	Suc01	0.05	12	342.3	342.3	0.146
34	Disaccharide	D-Lactose monohydrate	Lactose	Lac	0.5	12	360.31	342.3	0.146
35	Trisaccharide	D-Raffinose pentahydrate	Raffinose	Raf	0.5	18	594.5	504.42	0.099
36	Trisaccharide	D-Melezitose monohydrate	Melezitose	Mel	0.5	18	522.45	504.44	0.099
37	Arabinogalactan	Arabinogalactan	Arabinogalactan	Aran	0.5	–	–	–	–
38	Uridine	Uridine	Uridine	Uri	0.5	9	244.2	244.2	0.205
39	Mix	Mix	Mix	Mix	0.5	–	–	–	–
40	Water	Water	Water	Wat	–	–	–	–	–

Table S2. Carbon sources used in coculture experiment.

Data S1. kChip dataset. Each row represents a pairwise coculture. Interaction effect scores, classifications, type scores, and strength scores are calculated as described in the "Bootstrap resampling and interaction classification" section of the Materials and Methods.